Available online at www.sciencedirect.com
SCIENCE DIRECT®
Chemical Physics Letters 385 (2004) 8–11
CHEMICAL PHYSICS LETTERS
www.elsevier.com/locate/cplett

Wurtzite ZnS nanosaws produced by polar surfaces

Daniel Moore [a], Carsten Ronning [a,b], Christopher Ma [a], Zhong. L. Wang [a,*]

[a] Department of Materials, School of Materials Science and Engineering, Georgia Institute of Technology, 771 Ferst Dr, Atlanta, GA 30332-0245, USA
[b] II. Physikalisches Institut, Universität Göttingen, Tammannstr. 1, 37077 Göttingen, Germany

Received 12 November 2003; in final form 1 December 2003
Published online: 10 January 2004

Abstract

Wurtzite structured ZnS nanoribbons have been synthesized by a catalyst-free solid–vapor deposition technique. The nanoribbon has a saw-teeth shape, and the nanosaw is formed by a two-step process: a fast growth along *a*-axis forms the body of the saw; a subsequent growth along *c*-axis creates the teeth. The one-sided teeth structure is suggested to be the self-catalyzed growth of the Zn-terminated (0 0 0 1) surface, while the oxygen-terminated $(0\,0\,0\,\bar{1})$ surface is relatively chemically inactive. The growth of 'feather'-like structure of ZnS is also reported.

1. Introduction

The unique properties of quasi-1D nanostructures [1], such as nanobelts [2] and nanowires [3], make them an exciting field of interest with many possible applications. These materials have the potential to show novel or enhanced properties due to their decreased size, increased surface-to-volume ratio, and the novel morphologies. A wide range of techniques have been developed for the synthesis of 1D nanostructures, including solid–vapor deposition [2–4], lithography [4], laser ablation [5], sol–gel [6], and template-assisted methods [7,8].

Zinc sulfide, a direct wide band gap transparent semiconductor, is one of the most important materials used in photonics research [9–11]. It is also an important material for a variety of applications such as electroluminescent devices, solar cells, and other optoelectronic devices. One-dimensional nanostructures of ZnS are attractive because they are candidates for electronic and optoelectronic nanodevices [12,13]. Zinc blend and wurtzite structures are the two most popular structural configurations of ZnS. Single crystal zinc blend structured ZnS nanobelts have been synthesized by a solid–vapor phase process [14]. Nanostructured belts of zinc blend ZnS have been made through chemical conversion of ZnO nanobelts [15]. For technological applications, wurtzite is probably the most useful one because of its non-central symmetry and polar surfaces. In this Letter, we report the synthesis and characterization of wurtzite structured, polarization induced asymmetric growth of quasi-1D ZnS nanostructures, using a simple catalyst-free vapor deposition technique [16]. By presenting the structures of the observed 'saw'-teeth structure, the role played by polarity in the growth is demonstrated.

2. Experimental

Synthesis of ZnS nanostructure was achieved using a simple thermal evaporation process. Commercially available zinc sulfide (Alfa Aesar, 99.9% purity, metals basis) are placed in the center of an alumina tube inside of a horizontal tube furnace, where temperature, pressure, and evaporation time is controlled. The temperature is then raised to 1000 °C, as determined based on the melting temperature of zinc sulfide (1700 °C); the tube chamber pressure was kept at 300 mbar with a nitrogen flux at 50 sccm (standard cubic centimeters per minute). During evaporation, the product deposits onto a silicon substrate placed at the downstream end of the tube in a lower temperature zones. The evaporation time was ~10 min at the peak temperature.

* Corresponding author. Fax: +4048949140.
E-mail address: zhong.wang@mse.gatech.edu (Z.L. Wang).

0009-2614/$ - see front matter © 2003 Elsevier B.V. All rights reserved.
doi:10.1016/j.cplett.2003.12.063

3. Results and discussion

The sample was first analyzed by scanning electron microscope to determine the morphology of the deposited nanostructures. Fig. 1a shows a typical SEM image of the polar growth structures. Chemical analysis using the energy dispersive X-ray spectroscopy (EDS) (Fig. 1b) shows the stoichiometric phase of ZnS, while the oxygen and silicon signals come from the silicon substrate and silica surface layer on the substrate. There are two distinct classes of structures observed. One is the ribbon-like flat structure with one-sided teeth, named 'nanosaw'. The second structure observed is a 3D structure, with 'feathers' propagating off the main axis and separated circumferentially by 120°. Both of these samples were analyzed by TEM.

A low magnification TEM image of the saw structure is shown in Fig. 2a and the dark field image is given in Fig. 2b. The one-sided teeth structure of the saws is clearly seen. Electron diffraction (in Fig. 2c) reveals that the saws are single crystalline throughout the entire length. The diffraction also shows that the saw ribbon grows along $[2\bar{1}\bar{1}0]$ (the *a*-axis) and the teeth of the saw grow along [0001]. The teeth of the saw are different sizes, which indicate that they grow at different rates. The widths of the teeth range from ~5 to ~20 nm. It is important to note that the teeth grow out of the (0001) facet.

Structurally, the wurtzite ZnS crystal is described as a number of alternating planes composed of fourfold tetrahedral-coordinated S^{2-} and Zn^{2+} ions, stacked alternatively along the *c*-axis (Fig. 3). The wurtzite crystal structure has ±(0001) polar surfaces: the (0001) surface is terminated with positively charged Zn ions and the $(000\bar{1})$ surface is terminated with negatively charged S^{2-} ions. This creates positively charged (0001)-Zn and negatively charged $(000\bar{1})$-S polar surfaces. This polarity has been shown for ZnO, a typical wurtzite structure, to induce asymmetric growth of nanostructures due to differences in chemical activity between the two polar facets [16].

The saw-teeth structure is suggested to be a direct result from the difference in surface chemical activities as determined by surface termination. The Zn-terminated surface is chemically active, while the S-terminated surface is relatively inactive, resulting in the growth of the saw-teeth along [0001]. A powerful technique that can be applied to directly prove the termination of the

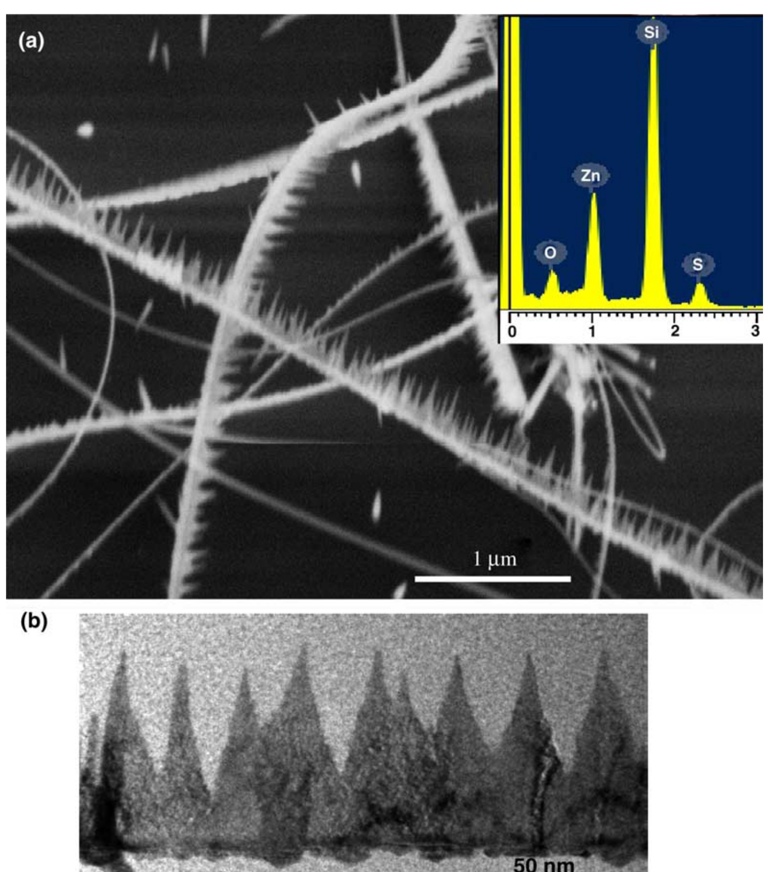

Fig. 1. (a) SEM image of the as-synthesized ZnS nanostructures. The inset is an energy dispersive X-ray spectrum recorded from the sample. (a) The Zn and S peaks are due to the nanostructures, while the silicon and oxygen peaks are due to the silicon substrate.

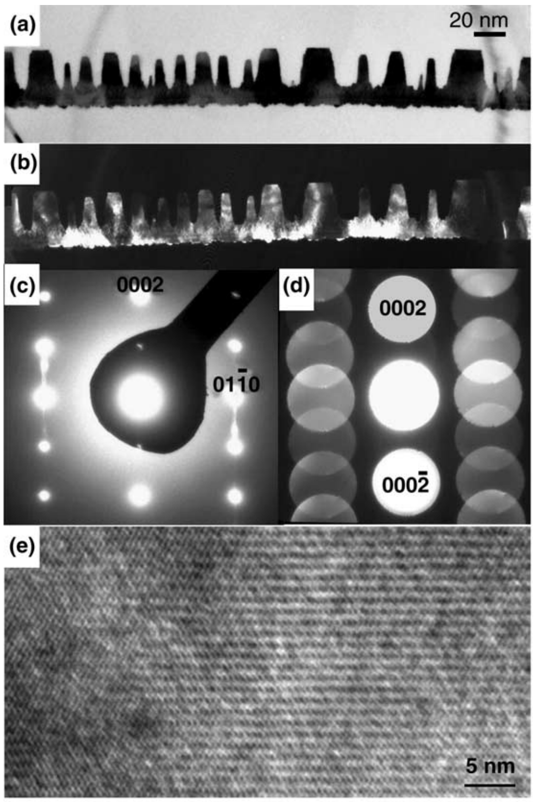

Fig. 2. (a) Bright field TEM image of a ZnS nanosaws. The polar growth occurs mainly on one side of the belt. (b) Dark field TEM image of the saw structure. (c) Diffraction pattern shows the saw ribbon is along [0 1 $\bar{1}$ 0] and the saw-teeth are along [0 0 0 1]. (d) CBED pattern recorded from the sample. (e) High-resolution TEM image recorded from the ZnS nanosaw.

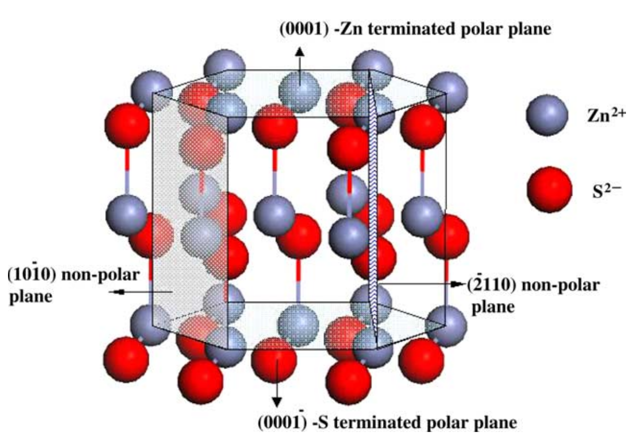

Fig. 3. Structure model of wurtzite ZnS.

surface is the convergent beam electron diffraction (CBED), but this technique requires the crystal being relatively thick. The CBED pattern recorded from a ribbon is shown in Fig. 2d, but the diffraction disks are featureless because the fact that the ribbon is thinner than the extinction distance for the ZnS (0 0 0 2) reflection, so that the dynamic diffraction effect is weak.

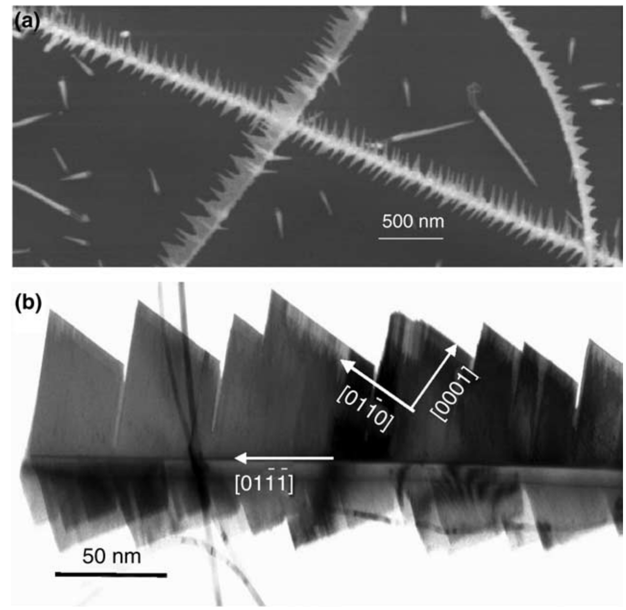

Fig. 4. (a) 'Feather' structure of ZnS. (b) A TEM image of the feather structure and the corresponding growth directions.

In Fig. 2e, a high-resolution TEM image recorded from the ribbon of the nanosaw is shown. The (0 0 0 1) lattice spacing is measured to be 0.61 nm, which is in agreement with bulk values of $c = 0.626$ nm. Based on the structural data presented here, the asymmetric growth features of the saw apparently result from the different growth rates on the (0 0 0 1)-Zn and the (0 0 0 $\bar{1}$)-S-terminated surfaces. The nanosaw is formed by a two-step process: a fast growth along [2 $\bar{1}$ $\bar{1}$ 0] forms the ribbon of the saw; a subsequent slower growth along [0 0 0 1] by a self-catalyzed process creates the teeth.

The second structure observed is the three dimensional 'feather' structures. Fig. 4a shows a low magnification SEM image of the structure. Electron diffraction pattern recorded from one side of the 'feather' shows that the wing grows along [0 0 0 1], and the center shaft is parallel to [0 1 $\bar{1}$ $\bar{1}$], as labeled in the TEM image in Fig. 4b. The other feathers are produced possibly because of bi-crystal growth.

4. Conclusion

In summary, we have presented the growth of two new nanostructures of wurtzite structured ZnS. The nanoribbon has a saw-teeth shape. The saw is formed by a two-step process: a fast growth along *a*-axis forms the body of the saw; a subsequent growth along the positive *c*-axis creates the teeth. The one-sided teeth structure is suggested to be the self-catalyzed growth of the Zn-terminated (0 0 0 1) surface, while the sulfide-terminated (0 0 0 $\bar{1}$) surface is relatively chemically inactive. The growth of 'feather'-like structure of ZnS is also reported. This study supports the proposal that surface polarity plays an important role in controlling the shapes of nanostructures in the wurtzite family.

Acknowledgements

Research was supported by the Georgia Tech NaST program and the Deutsche Forschungsgemeinschaft under grant Ro 1198/5-1.

References

[1] Z.L. Wang (Ed.), Nanowires and Nanobelts, Vol. I: Metal and Semiconductor Nanowires, and Vol. II: Nanowire and Nanobelts of Functional Oxides, Kluwer Academic Publisher.
[2] Z.W. Pan, Z.R. Dai, Z.L. Wang, Science 291 (2001) 1947.
[3] J. Hu, T.W. Odom, C.M. Lieber, Acc. Chem. Res. 32 (1999) 435.
[4] C. Ma, Y. Berta, Z.L. Wang, Solid State Commun., in press.
[5] X. Duan, C.M. Lieber, J. Am. Chem. Soc. 122 (2000) 188.
[6] F. Krumeich, H.J. Muhr, M. Niederberger, F. Bieri, B. Schyder, R. Nesper, J. Am. Chem. Soc. 121 (1999) 8324.
[7] C. Liu, J.A. Zapien, Y. Yao, X. Meng, C.S. Lee, S. Fan, Y. Lifshitz, S.T. Lee, Adv. Mater. 15 (2003) 838.
[8] X.D. Wang, P.X. Gao, J. Li, C.J. Summers, Z.L. Wang, Adv. Mater. 14 (2002) 1732.
[9] S. Kishimoto, A. Kato, A. Naito, Y. Sakamoto, S. Iida, Phys. Stat. Sol. 1 (2002) 391.
[10] L. Sun, C. Liu, C. Liao, C. Yan, J. Mater. Chem 9 (1999) 1655.
[11] X. Jiang, Y. Xie, J. Lu, L. Zhu, W. He, Y. Qian, Chem. Mater. 13 (2001) 1213.
[12] S. Gupta, J.C. McClure, V.P. Singh, Thin Solid Films 299 (1999) 22.
[13] W. Park, J.S. King, C.W. Neff, C. Liddell, C.J. Summers, Phys. Stat. Sol. 2 (2002) 949.
[14] C. Ma, D. Moore, J. Li, Z.L. Wang, Adv. Mater. 15 (2003) 228.
[15] X.D. Wang, J. Li, P.X. Gao, C.J. Summers, Z.L. Wang, Adv. Mater. 14 (2002) 1732.
[16] Z.L. Wang, X.Y. Kong, J.M. Zuo, Phys. Rev. Lett. 91 (2003) 185502.